energies

MDPI

Article

Biomass Polygeneration System for the Thermal Conversion of Softwood Waste into Hydrogen and Drop-In Biofuels

Lorenzo Bartolucci [1], Enrico Bocci [2], Stefano Cordiner [1], Emanuele De Maina [1,*], Francesco Lombardi [3], Vera Marcantonio [4,*], Pietro Mele [1], Vincenzo Mulone [1] and Davide Sorino [3]

1 Department of Industrial Engineering, University of Rome "Tor Vergata", Via del Politecnico 1, 00133 Rome, Italy
2 Department of Nuclear, Subnuclear and Radiation Physics, Marconi University, 00193 Rome, Italy
3 Department of Civil Engineering and Computer Science Engineering, University of Rome "Tor Vergata", Via del Politecnico 1, 00133 Rome, Italy
4 Unit of Process Engineering, Department of Engineering, University "Campus Bio-Medico" di Roma, Via Álvaro Del Portillo 21, 00128 Rome, Italy
* Correspondence: emanuele.de.maina@uniroma2.it (E.D.M.); v.marcantonio@unicampus.it (V.M.)

Abstract: In order to keep the +1.5 °C over-temperature, previously predicted with high confidence by IPPC Sixth Assessment, as minimal as feasible, it is more than vital to achieve a low-emission energy system. Polygeneration systems based on thermochemical processes involve biomass conversion in multi-output of bioenergy carriers and chemicals. Due to reduced energy input and input/output diversification, polygeneration energy systems are considered interesting pathways that can increase competitiveness of biomass-derived products. The proposed route of fast pyrolysis, sorption-enhanced biochar gasification and crude bio-oil hydrodeoxygenation to produce drop-in biofuel and hydrogen is examined. Both kinetic and equilibrium approaches were implemented in Aspen Plus to take into account the effect of the major operating parameters on the process performance and then validated against the literature data. Results show how the process integration leads to improved mass conversion yield and increases overall energy efficiency up to 10%-points, reaching the maximum value of 75%. Among the various parameters investigated, pyrolysis temperature influences mainly the products distribution while Steam/Biochar and Sorbent/Biochar affect the energy conversion efficiency.

Keywords: polygeneration energy systems; residual biomass valorization; biomass system modeling; fast pyrolysis; integrated sorption-enhanced gasification (ISEG)

check for updates

Citation: Bartolucci, L.; Bocci, E.; Cordiner, S.; De Maina, E.; Lombardi, F.; Marcantonio, V.; Mele, P.; Mulone, V.; Sorino, D. Biomass Polygeneration System for the Thermal Conversion of Softwood Waste into Hydrogen and Drop-In Biofuels. *Energies* **2023**, *16*, 1286. https://doi.org/10.3390/en16031286

Academic Editor: Dimitrios Sidiras

Received: 21 December 2022
Revised: 15 January 2023
Accepted: 18 January 2023
Published: 25 January 2023

Copyright: © 2023 by the authors. Licensee MDPI, Basel, Switzerland. This article is an open access article distributed under the terms and conditions of the Creative Commons Attribution (CC BY) license (https://creativecommons.org/licenses/by/4.0/).

1. Introduction

The last emission gap report states a current gap of 23 gigatons of CO_2 equivalent of a year to get back in line with the targets set in the IPPC Sixth Assessment [1]. If the measures announced by the countries are applied correctly, global warming at the end of the twentieth century will exceed 1.5 °C and is expected to settle around 2.6 °C. Hence, the urgent need to create a strategy for the transition to a resilient low-emission energy system has been very clear [1].

The transport sector is the second largest source of energy-related CO_2 emissions worldwide and has the highest level of reliance on fossil fuels of any sector, requiring a great economic and technological effort in the decarbonization of heavy-duty trucks, aviation and shipping [2]. In this context, the revised renewable energy directive (RED II) requires a minimum share of 14% of renewable energy in road and rail transport by 2030 [3]. Furthermore, the package 'Fit for 55%' [4] t sets the main targets of energy transition targets for 2030, and with its regulatory proposals 'New infrastructure for alternative fuels' [5], "ReFuelEU More sustainable aviation fuels" [6] and 'FuelEU: Cleaner maritime fuels" [7], it outlines the paths to achieve the energy transition in the transportation sector. Among

all the initiatives in the package, those related to emission reductions in shipping and the integration of sustainable aviation fuels (SAF) are the most remarkable. They are ambitious and set target schedules, which will end in 2050 with a 63% SAF integration and a 75% reduction in carbon intensity for maritime transport compared to the 2020 levels [8].

Bio-based fuels are currently available as alternative solutions to fossil-based fuels [9]. Biofuels can provide a fast and effective response to mitigate emissions. In fact, biofuels have properties similar to those of fossil fuels, and they can be used right away, without significantly impacting facilities and transportation vehicles [10]. However, biofuels must come from residual feedstock and non-competitive with food uses, in accordance with the requirements contained in Part A of Annex IX of RED II [3].

For the conversion of biomass feedstock to SAF, various pathways are possible, such as hydroprocessing, thermochemical processes, known as biomass-to-liquid (BtL), and biochemical processes.

In hydroprocessing, glyceride-based oils/fats are converted into a mixture of hydrocarbons (n-alkanes, iso-alkanes, and branched alkanes) in the same carbon range as fossil kerosene [10,11]. Currently, only renewable jet (HRJ) biofuels have reached the technological readiness to be commercialized, while BtL fuels are considered a promising alternative [12].

Among BtL processes, gasification and Fischer-Tropsch synthesis (FTS) are mature production routes, close to a commercial operation [13]. FTS consists of a heterogenous catalyzed process in which carbon monoxide is polymerized to a variety of linear hydrocarbons, called synthetic paraffinic kerosene (SPK), and water under a pressurized hydrogen atmosphere.

However, both HRJ fuels and SPK lack sufficient amounts of cyclic alkane and polycyclic aromatic hydrocarbons; both classes are required to increase the density and decrease the freezing point while ensuring proper valve sealing, respectively [14]. Thus, a low concentration of such hydrocarbon classes poses a limit to the blend ratio of SAF with conventional fossil-based kerosene [14].

Fast pyrolysis is a thermochemical process used to convert biomass under an inert atmosphere into tri-state products—bio-oil, biochar and a mixture of non-condensable gases.

Bio-oil-to-transportation fuel is limited by its high water content, the presence of oxygenated compounds, high viscosity, high acidity, poor stability, and reduced high heating value, making it unsuitable for direct engine applications [11].

Bio-oil upgrading can be carried out with different processes characterized by various technologies and the degree of complexity, including solvent addition, catalytic cracking, and distillation [15]. Among the upgrading processes, hydrodeoxygenation (HDO) carried out in the pressure range of (100–250 bar) and at high temperature (250–400 °C) in the presence of an appropriate catalyst is considered the most promising option due to the high conversion efficiency and high quality of the final products. Moreover, several studies show that upgraded bio-oils have a high concentration of monocyclic and polycyclic aromatics and compounds of chemical classes that are otherwise difficult to obtain with other technologies [16,17]. However, process severity and hydrogen consumption are technical, and economic barriers pose a limit to the industrial development and scale-up of the process [16].

Polygeneration systems based on thermochemical processes involve biomass conversion in multi-output of bioenergy carriers and chemicals. Due to reduced energy input and the diversification of input/output, polygeneration energy systems are considered interesting pathways to increase the competitiveness of biomass-derived products [17].

As stated in T. Nguyen et L. Clausen in [17], hydrogen production costs deeply influence the economics of the polygeneration system. Steam gasification is a thermochemical process used to convert biomass into a gas, called syngas, mainly composed of H_2, CO, CO_2 and CH_4 [18]. A common way to reduce the amount of CO_2 and increase the H_2 concentration is by means of the bed material acting as carbon dioxide sorbent for in situ CO_2 removal. This process is called a sorption-enhanced gasification process (SEG), and, by

reaction the shifting of the water gas shift towards equilibrium, it leads to higher hydrogen yields [19]. Generally, calcium oxide-based sorbents are used for the SEG process, and the exothermic carbonation reaction for CO_2 absorption is favored between 650 °C and 750 °C [19].

$$CaO_{(s)} + CO_2 \rightarrow CaCO_{3(s)} \quad \text{Absorption reaction}$$

In addition to the main products listed above, syngas also contains undesired organic compounds (tar) and inorganic contaminants, mainly hydrogen sulfide and hydrogen chloride, the quantity of which is related to the feedstock, the process conditions and the gasifier design [20–22]. These contaminants are a major risk factor for the lifetime of plant equipment; in fact, chlorine compounds may cause corrosion of metal equipment, health problems and environmental issues, while sulfur compounds may cause poisoning of the catalyst [22]. This is the reason why these contaminants must be reduced to below the common level of 1 ppm [22], which is suitable for the most common syngas applications (solid oxide fuel cell, an internal combustion engine, gas turbine, etc.).

The modeling of integrated thermochemical processes has been deeply considered in the literature as a powerful tool for estimating energy yield and process efficiencies when comparing different processes [17].

The Danish University of Aalborg and the Technical University of Denmark have worked in the past years on the conceptualization of a polygeneration system to valorize lignocellulose biomasses into electricity and biobased liquid fuels, such as methanol, through an integrated thermochemical system [23]. The integrated model consists of a gasification section, composed of a pyrolizer, a tar reformer, a char gasifier, and reversible solid oxide fuel cells (SOFC)—and a methanol synthesis section, composed primarily of a methanol reactor and a distillation unit. They found that the overall maximum efficiency of 70.5% was achieved by including a complete methanol production process while the efficiency in the case of electricity production was limited to 37%. Furthermore, the main challenge highlighted in the cited is to operate the SOFC with cleaned pyrolysis gas due to technical issues due to tars and hydrocarbons affecting the durability of the SOFC.

T. Nguyen and L. Clausen proposed novel polygeneration concepts based on catalytic hydropyrolysis for the conversion of woody biomass to deoxygenated bio-oils, synthetic natural gas, and methanol [17]. Among the various layouts they proposed, a conversion biomass pathway based on hydropyrolysis and hydrodeoxygenation, biochar gasification and extra hydrogen production led to a total system efficiency of 71% and a carbon conversion efficiency of 49% [17].

M. Prestipino et al. conducted an analysis of a system for the production of hydrogen, electricity, and heat using citrus peel as feedstock [24]. They started from the experimental data obtained in previous works and used them for the validation of the model developed in AVEVA PROII software [23]. The system included an air-steam gasifier, a pressure swing adsorption unit for hydrogen separation, and an internal gas engine for thermal power production. They found that under optimized operating conditions, the system had the highest hydrogen yield of 40 kg H_2/tdb, 1793 MJ/tdb (tons dry basis) of net electricity production and around 35% of global energy efficiency.

Lee et al. modeled a torrefaction/DFB steam gasification integrated system and investigated the effect of steam to biomass ratio (S/B) and the torrefaction temperatures on the syngas composition and cold gas efficiency (CGE) [25]. They found that torrefaction had a positive effect on cold gas efficiency, whereas an increase in gasification temperature and steam-to-biomass ratio led, respectively, to a decrease and an increase of CGE with an optimal value of approximately 74%.

In this study, we propose an integrated thermochemical process in which residual lignocellulosic biomass is converted to energy carriers, such as biodiesel, bio-gasoline and hydrogen through a conversion system based on low-temperature fast pyrolysis as a biomass pretreatment process to obtain biochar and bio-oil as intermediate bioenergy carriers. Hereafter, biochar is gasified, and the hydrogen produced, separated with a catalytic Pd-based membrane, is supplied for the bio-oil hydrodeoxygenation step to obtain

advanced biofuels. In addition to liquid biofuels, the polygeneration system produces extra hydrogen and syngas, which add value and diversification to the energy output.

The aim of this study is to evaluate the mass and energy conversion of the proposed pathway and to understand the feasibility of the approach, with particular attention to raw material consumption, mass and energy yields, and cold product efficiency. The process is evaluated using Aspen Plus software by means of a mix of kinetic and equilibrium modeling approaches to obtain the best compromise between the reliability and accuracy of the results and a limited complexity and computational cost.

2. Materials and Methods

The integrated thermochemical approach is evaluated by developing a numerical model in Aspen Plus software from AspenTech®. This software is widely used in the biomass energy upgrading system focused on the gasification step, while the proposed system integrates it into a wider conversion layout in order to achieve a polygeneration apparatus. Figure 1 shows a simplified layout of the proposed conversion plant.

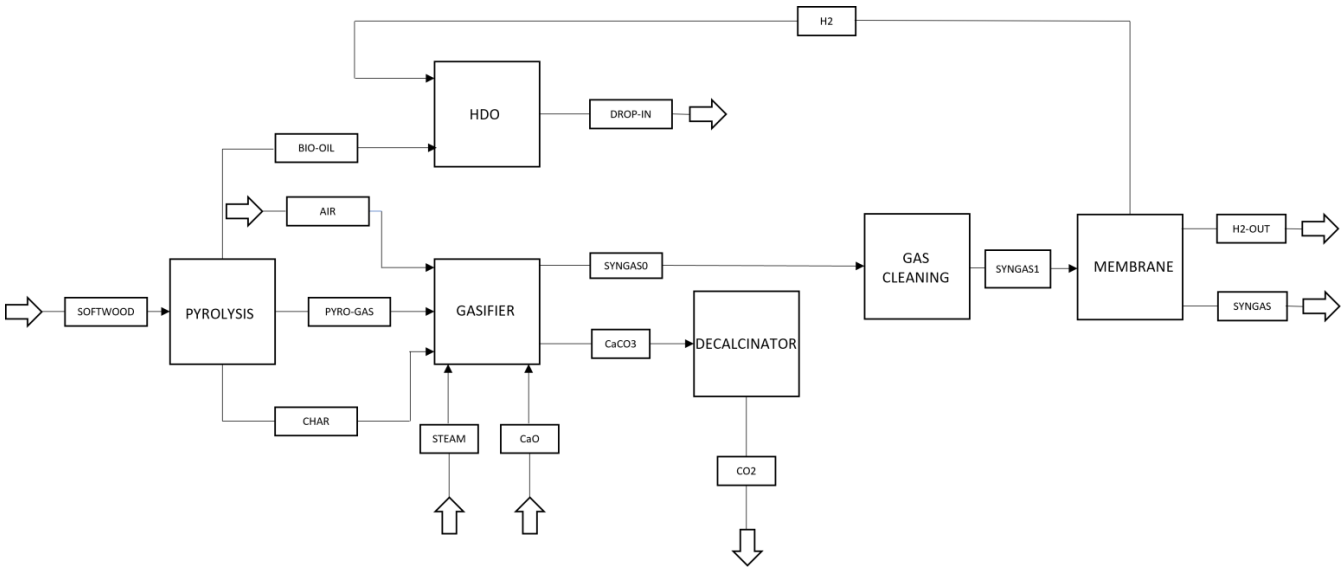

Figure 1. System layout.

In the following sections, a description of the system is given. Each section presents a component of the conversion plant and its modeling to describe its main purpose in the overall system, as well as hypotheses, assumptions, and literature references.

2.1. Feedstock

Feedstock lignocellulosic biomass has been selected in accordance with the EU Directive [3] and the scientific literature to avoid any competition with the food sector.

Among the spectrum of lignocellulose biomasses, softwood has been selected for the proposed work because of its wide availability and its valuable properties, which makes it a suitable feedstock for the proposed integrated conversion process. The characterization of softwood is reported in Table 1, according to [26,27].

2.2. Pyrolysis

Pyrolysis is the first step of biomass energy conversion, and its products are used in different sections of the system for further upgrading. It is modeled by an Aspen Plus kinetic model based on the approach proposed by Ranzi et al. and incorporates more than 50 species and 32 reactions [28,29].

Table 1. Characterization of softwood: elemental and proximate analysis, determination of low heating value and polymeric composition.

Parameter	Unit	References
C	50.7 w% $_{db}$	[26]
H	5.9 w% $_{db}$	[26]
N	0.2 w% $_{db}$	[26]
O	43.0 w% $_{db}$	[26]
S	0.005 w% $_{db}$	[26]
Cl	0.005 w% $_{db}$	[26]
Volatiles	85.4 w% $_{db}$	[26]
Fixed C	14.6 w% $_{db}$	[26]
Ash content	0.2 w% $_{db}$	[26]
Water content	7.2 w% $_{db}$	[26]
LHV (dry)	18.9 [MJ $kg_{db}{}^{-1}$]	[26]
LHV (moist)	17.4 [MJ kg^{-1}]	[26]
Cellulose	44%	[27]
Hemicellulos	24%	[27]
Lignin	32%	[27]

The input of the model is the biochemical biomass composition in terms of cellulose, hemicellulose, and lignin. This is converted into char, bio-oil, and syngas by a multistep kinetic mechanism that involves global and apparent first-order reactions. The upgrading of the bio-oil through the tile part of products is represented by 29 species, including gases and condensable species (bio-oil), and the solid part (biochar) made up of the sum of pure carbon, the unreacted part of biomass, and pseudo-species called 'metaplastics'. These metaplastic compounds have the role of representing the oxygenated and hydrogenated groups that are usually bonded to the carbonaceous matrix of biochar produced by the pyrolysis process.

The products of pyrolysis follow different routes in the system.

Vapors and non-condensable gases leaving the pyrolysis reactor undergo condensation. In detail, they enter a heat exchange to cool down to room temperature, 25 °C.

Condensable species, which form the bio-oil, include mainly phenols, alcohols, ketones, aldehydes, lignin-derived acids, sugar derivatives, water, and aromatics, according to data reported by other analytics [30–33].

Non-condensable gases pass through the condensation section and go beyond reaching the gasification section.

The solid part goes to an ideal separator, which allows it to obtain its elemental composition (C, H, O). The algorithm to convert species to elemental terms is implemented in Microsoft Excel, integrated with the process simulator using the Aspen Simulation Workbook.

The pyrolizer is modeled in Aspen Plus as a continuous stirred tank reactor with a feedstock residence time of 10 s.

Pyrolysis Validation

Although the pyrolysis model is based on an already validated model [29], validation of its implementation in the Aspen Plus software has been performed. For the pyrolysis model validation, two different aspects have been considered: the yield of the three output products and the elemental composition of the char.

For the validation of product yields, the work of S.S. Liaw et al. has been taken as a reference [34]. The Douglas fir wood composition was taken in terms of cellulose, hemicellulose, and lignin, and also the temperature and residence time of the pyrolysis.

By comparing the results of the model results and the reference presented in Figure 2, the model shows good agreement in terms of both the product distribution and temperature trends.

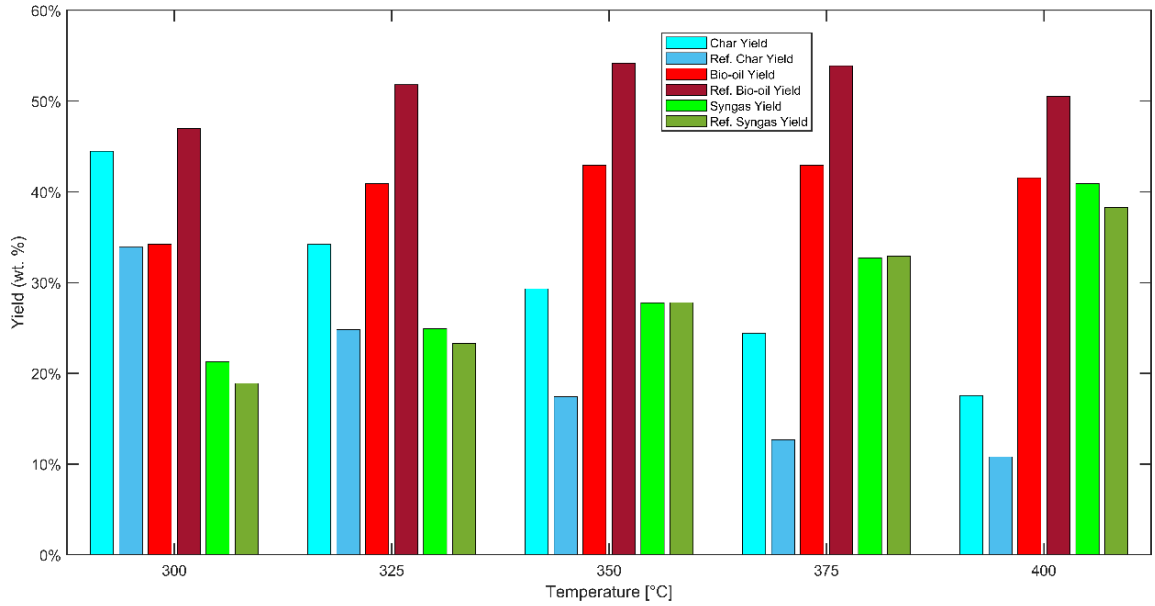

Figure 2. Validation of pyrolysis product yields—comparison with [34].

For the validation of the char composition, the work of X. Cao et al. [35] has been considered.

Since the article did not contain information on the characterization of the feedstock in terms of cellulose, hemicellulose, and lignin, data relative to maple wood have been taken from [36] while the temperatures and residence time of the pyrolysis processes have been taken equal to those reported in the article.

The results are synthesized in Figure 3 where a good prediction capacity of the model on char composition can be observed, with respect to the data given in the reference [35].

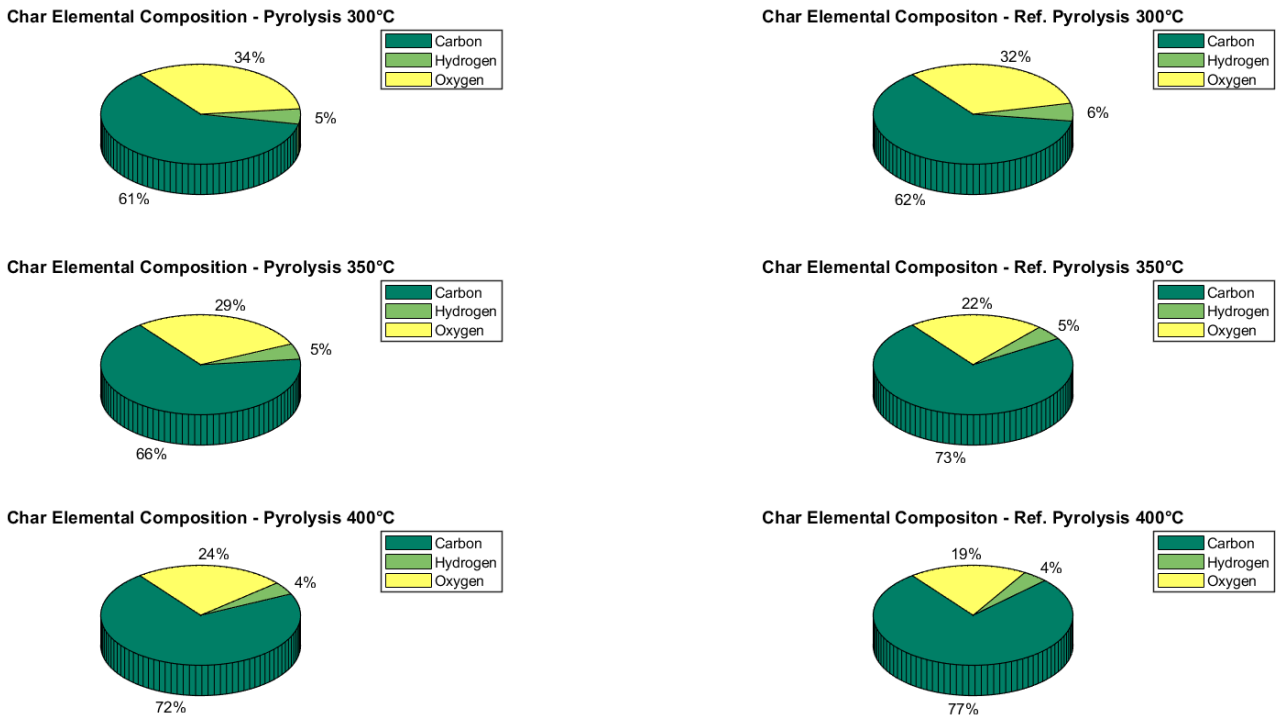

Figure 3. Validation of char elemental composition with variations in pyrolysis temperature. Validation by [35].

2.3. Gasifier

The simulation of the sorption-enhanced char gasification process is based on mass and energy balances and chemical equilibrium among all processes.

The temperature of the gasification process is set at 650 °C. The gasifier is fed with CaO for in situ CO_2 adsorption. The oxidizing agent is a mixture of steam and air. Both the steam/char and CaO/char feeding of the system are considered as variable operating parameters, and sensitivity to these is presented in the results section.

Reactions modeled for the sorption-enhanced gasification are listed in Table 2.

Table 2. Gasification reactions [37,38].

Reaction	Reaction Name	Heat of Reaction	Reaction Number
Heterogeneous reaction			
$C + 0.5\ O_2 \rightarrow CO$	Char partial combustion	(-111 MJ kmol^{-1})	(R1)
$C + H_2O \leftrightarrow CO + H_2$	Water–gas	(+172 MJ kmol^{-1})	(R2)
$2\ CO \leftrightarrow CO_2 + C$	Boudouard	(+172 MJ kmol^{-1})	(R3)
Homogeneous reactions			
$H_2 + 0.5\ O_2 \rightarrow H_2O$	H_2 partial combustion	(-283 MJ kmol^{-1})	(R4)
$CO + H_2O \leftrightarrow CO_2 + H_2$	Water–gas shift	(-41 MJ kmol^{-1})	(R5)
$CH_4 + H_2O \rightarrow CO + 3H_2$	Steam-methane reforming	(+206 MJ kmol^{-1})	(R6)
$CaO + CO_2 \leftrightarrow CaCO_3$	Carbonation	(-179 MJ kmol^{-1})	(R7)

As already reported in the Pyrolizer section, the kinetic approach for pyrolysis modeling allows obtaining a high level of detail on the char elemental composition and delves deeper into the common assumption of char composed of only carbon performed in other studies of two-step gasification in Aspen Plus [39,40].

The gasifier is modeled as a Gibbs reactor through restricted chemical equilibrium [37,39,41] while tar formation is evaluated in a separate reactor, a RYield, taking a fraction of C and H_2 and converting them into tar. Tar is divided into 60% benzene, which does not condensate, 20% toluene (as a representative of fast tar) and 20% naphthalene (as representative of the slow tar) according to reference [42].

Gasification Validation

The sorption-enhanced steam gasification process model has been validated for its prediction capacity of syngas volume fraction composition.

The work of J.C. Schmid et al. [19] was used as a reference. In their study, the performance of a dual fluidized bed-enhanced steam gasifier was evaluated. The reference case using lignite was taken into account because it was considered the most similar to the biochar used in this work. The feedstock characteristics and the operating conditions of J.C. Schmid's work were imposed into the gasification model in Aspen Plus.

The comparison of the reference results and the prediction of the proposed model presented in Figure 4 shows a good agreement.

2.4. Gas Cleaning

Syngas purification is achieved by hot gas cleaning processes, including dolomite in the bed, catalytic filter candles in the freeboard of the reactor for tar removal, and two sorbent reactors for H_2S and HCl removal. The in-bed dolomite for tar removal was simulated as a Gibbs reactor by imposing fractional conversion from the literature [21]. The catalytic candles were modeled as stoichiometric reactors, and the reactions that occurred inside and the conversion rates were set according to experimental data by Savuto et al. [43]. The adsorption of H_2S was simulated using an equilibrium reactor, the temperature was set at 450 °C, and ZnO was used as a sorbent (ZnO: H_2S was 2) [21]. HCl adsorption was simulated using a Gibbs reactor, the temperature was set at 550 °C, and nacholite was used as sorbent [44].

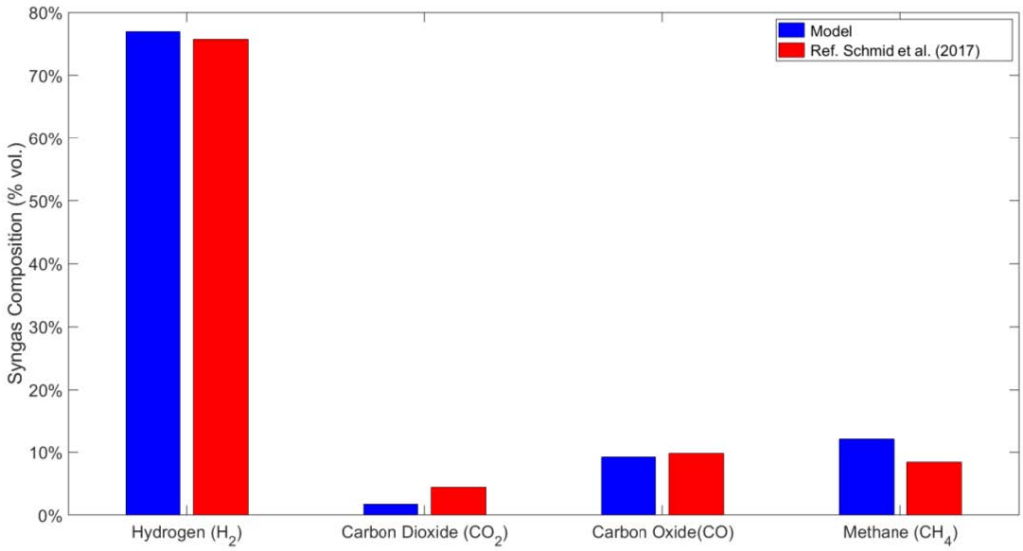

Figure 4. Validation of sorption-enhanced gasification: syngas composition of char gasification at 650 °C, S/B = 1 [19].

The effectiveness of gas cleaning is demonstrated in Table 3 since the level of inorganic contaminants decreased to less than 1 ppm and the level of tar decreased to less than 1 g/Nm^3, which is the limit level for the most common applications of syngas [21].

Table 3. Syngas composition.

	SYNGAS,0 (Out of SEG)	SYNGAS,1 (Out BEDREACT)	SYNGAS,2 (Out CANDLE)	SYNGAS,3 (Out H2S Removal)	SYNGAS,4 (Out HCl Removal)
H_2 [$\%_{vol,dry}$]	80.17	80.17	83.87	83.87	83.87
CO [$\%_{vol,dry}$]	6.24	6.24	11.5	11.5	11.5
CO_2 [$\%_{vol,dry}$]	1.18	1.18	0.98	0.98	0.98
CH_4 [$\%_{vol,dry}$]	12.45	12.45	3.6	3.6	3.6
C_6H_6 [g/Nm^3]	21.15	5.28	1.56	1.56	1.56
C_7H_8 [g/Nm^3]	8.60	1.63	0.45	0.45	0.45
$C_{10}H_8$ [g/Nm^3]	11.57	2.05	0.62	0.62	0.62
H_2S [ppm]	1200	200	180	0.04	0.04
HCl [ppm]	750	105	100	0.03	0.03

2.5. Hydrodeoxygenation

The condensable species produced by the pyrolysis process have a high oxygen content (about 50%); therefore, these are not suitable for direct energy use. The oxygen content is reduced by an HDO reactor. It consists of three main sections: hydrotreating, distillation, and hydrocracking. All three processes are enabled by the presence of hydrogen (approximately 0.06 $kg_{H2}/kg_{bio\text{-}oil}$) that is taken from the post-gasification syngas through a membrane separator reactor [45]. The HDO modeling is based on the work of J.F. Peters [46].

2.5.1. Hydrotreatment

The hydrotreatment section consists of two stages characterized by different operating conditions. The first stage is a mild hydrotreatment, where the hydrogen pressure is 170 bar and the working temperature is 270 °C. Some catalysts are usually present in the reactor to ensure the effectiveness of this process, for example, the Co-Mo catalyst [47]. In mild HDO, extremely unstable compounds (such as acidic oxygen compounds) react to give rise to more stable products. This stage also produces water that is separated to enhance the energy density. The modeling is based on the chemical compound approach, where the condensable species are grouped in reference model compounds (for example, phenols,

ketones, etc.). [48] and then converted to the resulting species by the Aspen Plus RYield components. The result is a stabilized oil with still elevated oxygen concentration (about 30%), which is not yet sufficient. Therefore, another hydrotreatment stage is necessary, i.e., deep hydrodeoxygenation. In this second stage, the hydrogen pressure is 140 bar and the working temperature is 303 °C, ensuring the conversion of high oxygen content products into high-carbon and hydrogen chemical compounds, such as linear and cyclic alkanes and aromatic hydrocarbons, calculated using the model presented in [49].

2.5.2. Distillation

The purpose of the distillation section is to separate the heavier compounds from the more volatile ones to obtain two different drop-in fuels: gasoline and diesel. A mixture of hydrotreatment outlput, hydrogen and hydrocracking output enters the inlet of the first distillation column at a temperature of 157 °C and a pressure of 15 bar. A stream of typical gasoline compounds leaves the column head while the heavier compounds come out from the bottom, which is depressurized to 0.1 bar. These heavier compounds enter the second distillation column, which allows obtaining diesel-like fuel at the top, while the heavier compounds reach the hydrocracking reactor inlet at the bottom.

2.5.3. Hydrocracking

The final step of the HDO section is hydrocracking. Its purpose is to break down the heavier part, which is not suitable for direct application. This heavy fraction is first pressurized up to 60 bar, mixed with hydrogen, and heated to a temperature of 600 °C. In the hydrocracker, the inlet flow is represented by chrysene. It reacts with hydrogen and produces linear and cyclic alkanes and aromatic hydrocarbons, such as benzene and toluene. The products leaving the reactor are then depressurized, cooled to a temperature of 32 °C, and enter the flash chamber along with the hydrotreating products, thus closing the cycle. The reactions accounted for in the model are reported in Table 4.

Table 4. Hydrocracking reactions.

Reaction	Reaction Number
Chrysene + 3 H_2 → Naphthalene + M-Xylene	(R8)
Chrysene + 10.1 H_2 → 0.35 Benzene + 0.25 Dodecane + 0.32 Isopropylbenzene + + 0.32 Methylcyclohexane + 0.32 Ethane + 0.33 Toluene + 0.43 Undecane + 0.1 CH_4	(R9)
Chrysene + 11 H_2 → Cyclohexane + Bicyclohexyl	(R10)
Chrysene + 13 H_2 → 0.35 N-octadecane + 0.33 Isopropylcyclohexane + + 0.33 N-nonane + 0.32 Cyclopentane + 0.32 N-tridecane	(R11)
Chrysene + 14.25 H_2 → 0.5 Pentane + 0.5 N-octane + 0.25 Methylnonane + + 0.5 N-pentadecane + 0.5 Propane	(R12)
Chrysene + 15.6 H_2 → Butane + 0.8 Tetradecane + 0.2 N-hexane + 1.6 CH_4	(R13)

An example of the concentration of carbon, hydrogen and oxygen before and after hydrodeoxygenation with their respective low heating values are shown in Table 5.

Table 5. Oil characteristics before and after hydrodeoxygenation.

	Pre HDO	Post HDO
C (% wt.)	56.2	85.5
H (% wt.)	6.1	14.3
O (% wt.)	37.7	0.2
LHV (MJ/kg)	18.5	46.3

3. Results and Discussion

The thermochemical integrated system is evaluated under different operating conditions to understand its effects on the conversion process performance.

The Key Performance Indicators (KPIs) used for the analysis are defined according to the following equations:

$$\eta_{overall} = \frac{m_{hydrogen}LHV_{hydrogen} + m_{drop\ in}LHV_{drop\ in} + m_{syngas}LHV_{syngas}}{m_{biomass}LHV_{biomass} + Pw_{pyrolysis} + Pw_{SEG} + Pw_{HDO} + Pw_{gas\ cleaning}} \quad (1)$$

$$Energy\ Yield_i = \frac{m_i \cdot LHV_i}{m_{biomass} \cdot LHV_{biomass}} \quad (2)$$

$$Mass\ Yield_i = \frac{m_i}{m_{biomass}} \quad (3)$$

These parameters were chosen because they have already been assessed according to the literature [23].Overall efficiency indicates the performance of the entire system and takes into account the power consumption of all processes in addition to the biomass input power.On the other hand, the energy yield takes into account the input biomass energy content to represent how it is distributed in the final products.Finally, the mass yield gives information about the material redistribution of the biomass input.

The effects of three main operating parameters are studied: the pyrolysis temperature, the steam/char ratios, and the CaO/char ratios in the gasifier.

The operating conditions considered are as follows:

- Four pyrolysis conditions: no pyrolysis, T_{pyro} = 300 °C, T_{pyro} = 350 °C, T_{pyro} = 400 °C;
- Five CaO/char ratios: from 1 to 2 by step of 0.25;
- Ten steam/char ratios: from 0.2 to 2 in 0.2 steps.

The CaO/char range is chosen as a result of its effectiveness in the SEG process. In fact, the sorption of CO_2 under the gasifier in the chosen CaO condition displays good behavior. Figure 5 shows the H_2 and CO_2 dry molar fraction for different CaO/char ratios without pyrolysis and a steam/char of 0.4. Figure 2 shows between one and two values of CaO/char an increment of about 13% points is achieved in the H_2 molar fraction of dry syngas out of the gasifier and a plateau in CO_2 absorption is reached.

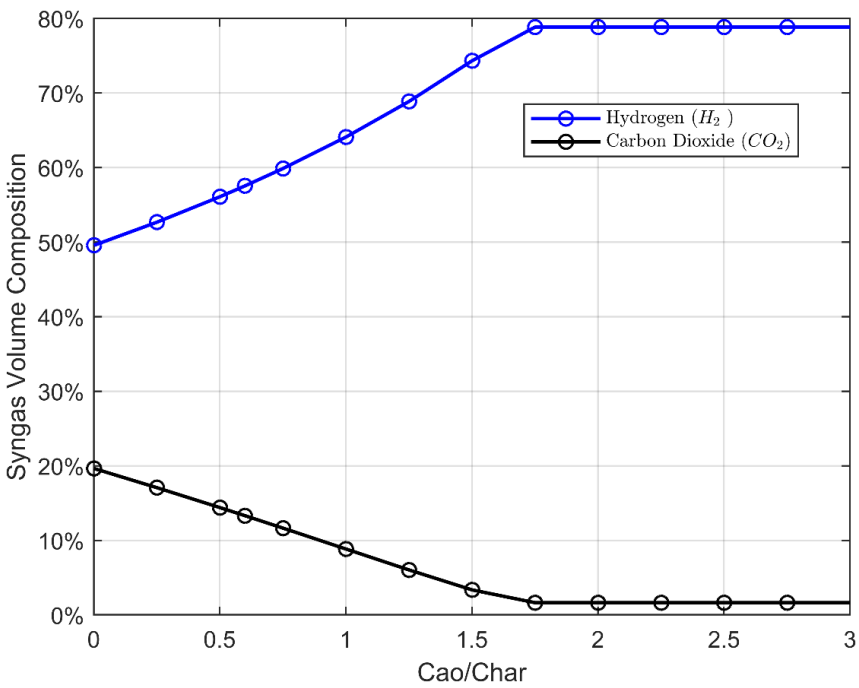

Figure 5. H_2 and CO_2 trend varying CaO to char ratio.

The results in terms of overall efficiency under the different tested conditions are reported in Figure 6, where the warmer colors represent higher efficiency values for the respective values of CaO/char and steam/char, and the black lines represent the iso-efficiency curves. A general trend can be observed in the results: by increasing the value of the steam/char ratio, the overall efficiency increases to a saturation value. A further increase leads to a monotonically decreasing trend, whose slope depends on the pyrolysis temperature. This trend highlights the occurrence of a peak, depending on both the pyrolysis temperature and the steam/char ratio. In particular, the peak value of the overall efficiency is moved to the right (higher S/C ratios) as the pyrolysis temperature is increased. This behavior occurs due to the increase in the concentration of char carbon with the pyrolysis temperature, as can be observed in Figure 3 in the Materials and Methods Section. As a result, greater CO production is obtained through the water gas reaction (R2), increasing the water consumption potential for the water gas shift reaction (R5). These considerations are consistent with the results presented in [25], which show a higher amount of carbon monoxide produced with the increase in torrefaction temperature implemented upstream of the gasifier.

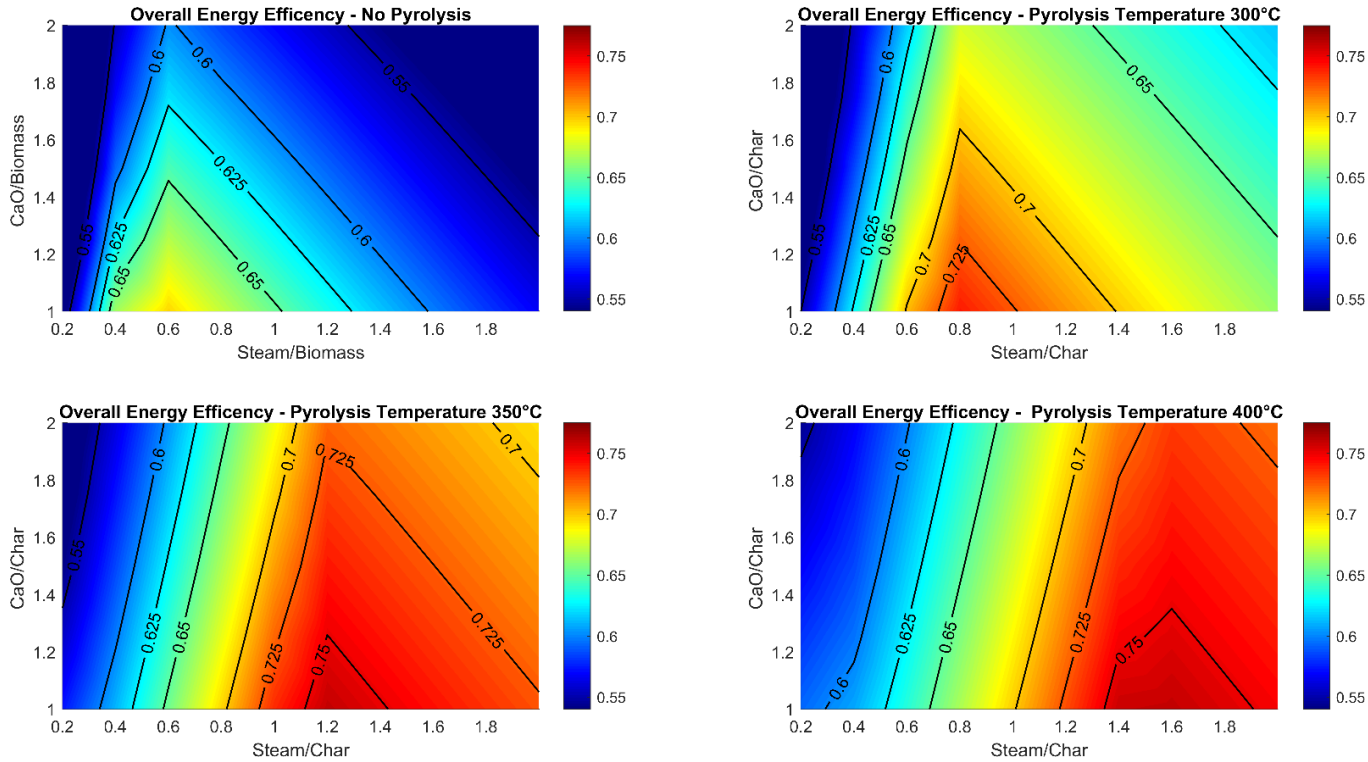

Figure 6. Overall energy efficiency as functions of the Steam/Char and CaO/Char ratios.

In general, a higher specific steam consumption appears to be profitable for the hydrogen production capacity of the system due to a higher pyrolysis temperature.

The energy yields and the overall efficiency as functions of the pyrolysis conditions are described in Figure 7a for the S/C ratio where the overall efficiency is maximized at the CaO / char ratio of 1.5. Peak efficiency is achieved for T_{pyro} = 400 °C, reaching a value of approximately 74% compared to the 64% obtained without pyrolysis pretreatment. This is due to the reduction of the lesser energy requirement in the gasifier, mainly for the steam generation and the $CaCO_3$ regeneration, and the increased drop-in fuel production capacity (due to the increase in the bio-oil fraction with the pyrolysis temperature). This increase in overall efficiency by char valorization is also reported in [17], where the gasification of the hydropyrolysis char increases the efficiency of the plant by approximately 13% compared to the case without char valorization.

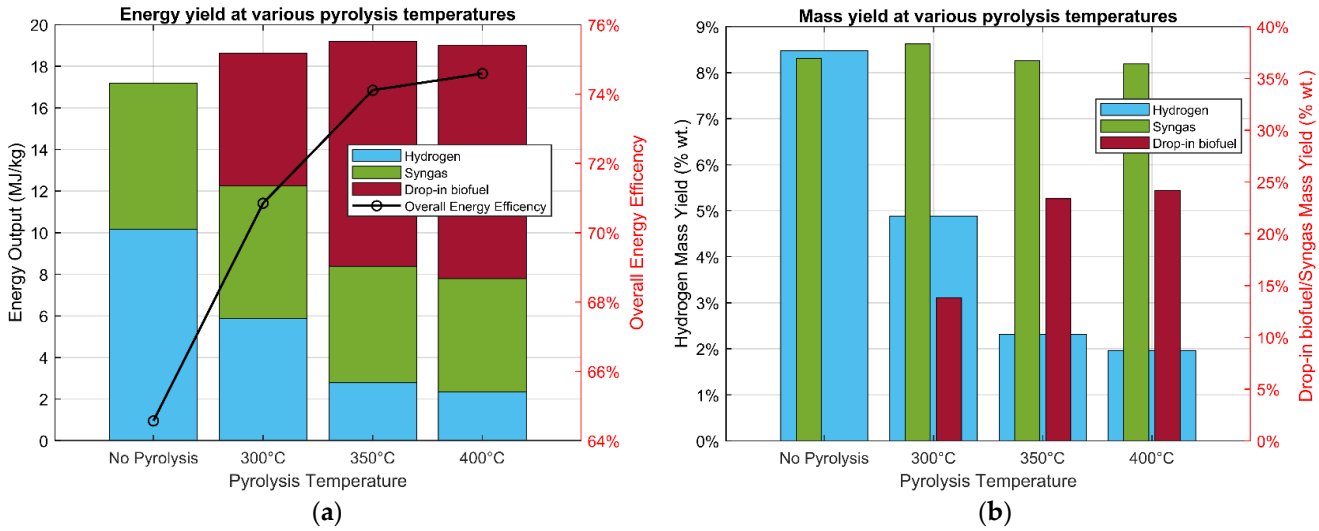

Figure 7. Performance parameters of the system (**a**) Energy output and overall energy efficiency as pyrolysis temperature changes (**b**) Mass output yields as pyrolysis temperature changes.

The overall efficiency versus the pyrolysis temperature behavior shows a sharp increase moving from the case of no pyrolysis up to the 350 °C case (about 10%) to reach a saturation close to a value of 74% for a further temperature increase. A decrease in the overall efficiency with higher temperature is expected due to the lower bio-oil production and, therefore, a reduction in the drop-in fuel production capacity. In addition, a further increase in the pyrolysis temperature is not expected to a lead to higher hydrogen yield due to the lower biochar availability to gasify. No significant increase in the hydrogen production capacity is expected, as the char production would decrease, reducing the hydrogen production. Two interesting operating points are observed in Figure 7a. One is at T_{pyro} 350 °C, where there is the maximum energy output (19.2 MJ/kg) but not the maximum efficiency (74.1%), and the other is at T_{pyro} 400 °C, which corresponds to a lower energy output (19 MJ/kg) but has the maximum energy efficiency (75%).

The mass yields of the output streams as the pyrolysis temperature changes are illustrated in Figure 7b. In the case of no pyrolysis and hydrodeoxygenation, thus pure gasification, there is a high hydrogen fraction (about 8%) and intermediate syngas (about 35%) yield. Further investigation of the output fluxes reveals that syngas yields are greater for the pyrolysis cases compared with no-pretreatment gasification, peaking at 60% in the case of 300 °C pyrolysis temperature pretreatment. Furthermore, with increasing temperature, there is a marked increase in biofuel drop-in products, with a maximum value of about 24% at 400 °C. This can be explained because the amount of bio-oil input at the HDO process increases with the pyrolysis temperature. Finally, the hydrogen yield is decreased with the pyrolysis temperature due to the demands of both the hydrotreating and the hydrocracking processes for higher bio-oil production.

The energy demands in each macroprocess are described in Table 6. Under the same conditions, that is, optimized steam/char and CaO/char fixed at 1.5, the most energy intensive condition turns out to be the no-pretreatment gasification case. In fact, as reported in Table 6, while the energy expenditure for biomass pretreatment is constant (evaluated according to the data reported in [49]), and the pyrolysis and the HDO processes consume a maximum of 3.35 MJ/kg together, sorption and enhanced steam gasification with $CaCO_3$ regeneration appear to be highly energy intensive. With pyrolysis and, thus, HDO, the energy expenditure for the gasification process is remarkably limited by reducing the mass flux at the gasifier. In fact, the high energy demand for the gasification process is due to two different factors: the heating demand for steam production at 650 °C and the energy demand for the decalcification process, in turn depending on the amount of CO_2 absorbed.

Table 6. Energy input (MJ/kg) at Steam/Biochar optimized and CaO/Char = 1.5.

	Pretreatment	Pyrolysis	Gasification	HDO	Total
No pyro	0.53	0	7.19	0	7.72
300 °C	0.53	0.65	4.74	1.49	7.41
350 °C	0.53	0.93	3.19	2.38	7.02
400 °C	0.53	1.03	2.68	2.32	6.57

4. Conclusions

In this study, an integrated thermochemical system for the polygeneration of energy carriers from biomass has been presented. The model has been developed and Aspen Plus software, with the main sections (pyrolysis and gasification) have been validated by the data from the literature. The main goal of the study was to evaluate the effectiveness of pyrolysis as a pretreatment for a subsequent SEG process toward the definition of a flexible integrated thermochemical plant for the production of multi-energy carriers (drop-in, hydrogen, and syngas).

The main findings of this study can be summarized as follows:

- The results of the analysis of the sensitivity of the steam/char, CaO/char and pyrolysis temperature showed that the pyrolysis pretreatment provides noteworthy advantages, including an increase in the overall energy efficiency (up to a pyrolysis temperature of 400 °C) and a diversification of the energy outputs, since a drop-in fuel with high heating value was obtained by upgrading the pyrolysis bio-oil;
- A correlation between the pyrolysis temperature and the steam/char ratio was found to influence the overall peak efficiency value. In particular, a set of optimal operating parameters toward energy efficiency is T_{pyro} = 400 °C, Steam/Char = 1.6 and CaO/Char = 1.5. At such optimal values, an overall efficiency of about 75% is obtained, with hydrogen, syngas, and drop-in mass yields of 2%, 34% and 26%;
- The maximum total output energy flux is obtained at T_{Pyro} 350 °C while hydrogen production capacity is maximized with reduced T_{Pyro}, with a peak without pyrolysis pretreatment at 8% hydrogen mass yield and 10 MJ/$kg_{biomass}$ energy yield;
- The system can be designed and operated flexibly according to different pyrolysis operating temperatures to maximize the production capacity of either biofuel or hydrogen or to maximize the energy efficiency of the overall process.

Ultimately, the proposed integrated approach shows how the synergy of the processes helps to improve the overall plant performance. In particular, the presence of pyrolysis as the first step, before the SEG, significantly increases the efficiency of the plant (about 10%).

Author Contributions: Conceptualization, E.B. and V.M. (Vincenzo Mulone); methodology, E.D.M., V.M. (Vera Marcantonio), P.M. and D.S.; software, E.D.M., V.M. (Vera Marcantonio), P.M. and D.S.; validation., E.D.M., P.M. and D.S.; formal analysis, E.D.M., P.M. and D.S.; investigation, E.D.M., P.M., D.S. and L.B.; data curation, E.D.M., P.M. and D.S.; writing—original draft preparation, E.D.M., P.M. and D.S.; writing—review and editing, S.C., L.B. and V.M. (Vincenzo Mulone); supervision, E.B., L.B., S.C., F.L. and V.M. (Vincenzo Mulone). All authors have read and agreed to the published version of the manuscript.

Funding: This research received no external funding.

Data Availability Statement: Not applicable.

Conflicts of Interest: The authors declare no conflict of interest.

References

1. United Nations Environment Programme. Emissions Gap Report 2022: The Closing Window—Climate Crisis Calls for Rapid Transformation of Societies. Nairobi. 2022. Volume 20, No. 2. Available online: https://www.unep.org/emissions-gap-report-2022 (accessed on 27 October 2022).
2. IEA. *World Energy Outlook 2021*; IEA Publications: Paris, France, 2021; p. 15. Available online: www.iea.org/weo (accessed on 1 October 2021).
3. EU. Directive (EU) 2018/2001 of the European Parliament and of the Council on the Promotion of the Use of Energy from Renewable Sources. *Off. J. Eur. Union* **2018**, *L328*, 82–209.
4. Erbach, G.; Jensen, L.; European Parliament. *Briefing towards Climate Neutrality: Fit for 55 Packagel*; European Parliamentary Research Service: Brussels, Belgium, 2022.
5. Soone, J. *Deployment of Alternative Fuels Infrastructure: Fit for 55 Package*; European Parliamentary Research Service: Brussels, Belgium, 2022.
6. Soone, J. *ReFuelEU Aviation Initiative: Sustainable Aviation Fuels and the Fit for 55 Package*; Think Tank | European Parliament: Brussels, Belgium, 2022.
7. Maritime, F. *EU Legislation in Progress Sustainable Maritime Fuels 'Fit for 55' Package: The FuelEU Maritime Proposal*; European Parliamentary Research Service: Brussels, Belgium, 2021.
8. dan Rosad, S. Proposal for a Regulation of the European Parliament and of the Council on ensuring a level playing field for sustainable air transport—'ReFuelEU Aviation'. *Suparyanto Dan Rosad* **2015**, *5*, 248–253.
9. Nadel, S. Electrification in the Transportation, Buildings, and Industrial Sectors: A Review of Opportunities, Barriers, and Policies. *Curr. Sustain. Energy Rep.* **2019**, *6*, 158–168. [CrossRef]
10. Panoutsou, C.; Giarola, S.; Ibrahim, D.; Verzandvoort, S.; Elbersen, B.; Sandford, C.; Malins, C.; Politi, M.; Vourliotakis, G.; Zita, V.E.; et al. Opportunities for Low Indirect Land Use Biomass for Biofuels in Europe. *Appl. Sci.* **2022**, *12*, 4623. [CrossRef]
11. Bashir, M.A.; Lima, S.; Jahangiri, H.; Majewski, A.J.; Hofmann, M.; Hornung, A.; Ouadi, M. A step change towards sustainable aviation fuel from sewage sludge. *J. Anal. Appl. Pyrolysis* **2022**, *163*, 105498. [CrossRef]
12. Chen, Y.-K.; Lin, C.-H.; Wang, W.-C. The conversion of biomass into renewable jet fuel. *Energy* **2020**, *201*, 117655. [CrossRef]
13. Dossow, M.; Dieterich, V.; Hanel, A.; Spliethoff, H.; Fendt, S. Improving carbon efficiency for an advanced Biomass-to-Liquid process using hydrogen and oxygen from electrolysis. *Renew. Sustain. Energy Rev.* **2021**, *152*, 111670. [CrossRef]
14. Díaz-Pérez, M.A.; Serrano-Ruiz, J.C. Catalytic Production of Jet Fuels from Biomass. *Molecules* **2020**, *25*, 802. [CrossRef]
15. Elkasabi, Y.; Mullen, C.A.; Boateng, A.A.; Brown, A.; Timko, M.T. Flash Distillation of Bio-Oils for Simultaneous Production of Hydrocarbons and Green Coke. *Ind. Eng. Chem. Res.* **2019**, *58*, 1794–1802. [CrossRef]
16. Lahijani, P.; Mohammadi, M.; Mohamed, A.R.; Ismail, F.; Lee, K.T.; Amini, G. Upgrading biomass-derived pyrolysis bio-oil to bio-jet fuel through catalytic cracking and hydrodeoxygenation: A review of recent progress. *Energy Convers. Manag.* **2022**, *268*, 115956. [CrossRef]
17. Nguyen, T.-V.; Clausen, L.R. Thermodynamic analysis of polygeneration systems based on catalytic hydropyrolysis for the production of bio-oil and fuels. *Energy Convers. Manag.* **2018**, *171*, 1617–1638. [CrossRef]
18. Marcantonio, V.; Ferrario, A.M.; Di Carlo, A.; Del Zotto, L.; Monarca, D.; Bocci, E. Biomass Steam Gasification: A Comparison of Syngas Composition between a 1-D MATLAB Kinetic Model and a 0-D Aspen Plus Quasi-Equilibrium Model. *Computation* **2020**, *8*, 86. [CrossRef]
19. Schmid, J.C.; Fuchs, J.; Benedikt, F.; Mauerhofer, A.M.; Müller, S.; Hofbauer, H.; Stocker, H.; Kieberge, N.; Bürgler, T. Sorption enhanced reforming with the novel dual fluidized bed test plant at tu wien. In Proceedings of the European Biomass Conference and Exhibition (EUBCE), Stockholm, Sweden, 12–15 June 2017.
20. Marcantonio, V.; De Falco, M.; Capocelli, M.; Bocci, E.; Colantoni, A.; Villarini, M. Process analysis of hydrogen production from biomass gasification in fluidized bed reactor with different separation systems. *Int. J. Hydrogen Energy* **2019**, *44*, 10350–10360. [CrossRef]
21. Marcantonio, V.; Müller, M.; Bocci, E. A Review of Hot Gas Cleaning Techniques for Hydrogen Chloride Removal from Biomass-Derived Syngas. *Energies* **2021**, *14*, 6519. [CrossRef]
22. Marcantonio, V.; Bocci, E.; Ouweltjes, J.P.; Del Zotto, L.; Monarca, D. Evaluation of sorbents for high temperature removal of tars, hydrogen sulphide, hydrogen chloride and ammonia from biomass-derived syngas by using Aspen Plus. *Int. J. Hydrogen Energy* **2020**, *45*, 6651–6662. [CrossRef]
23. Gottschalk, F.; La Rosa, M. Process Configuration. In *Modern Business Process Automation*; Springer: Berlin/Heidelberg, Germany, 2009; pp. 459–487. [CrossRef]
24. Prestipino, M.; Chiodo, V.; Maisano, S.; Zafarana, G.; Urbani, F.; Galvagno, A. Hydrogen rich syngas production by air-steam gasification of citrus peel residues from citrus juice manufacturing: Experimental and simulation activities. *Int. J. Hydrogen Energy* **2017**, *42*, 26816–26827. [CrossRef]
25. Bach, Q.-V.; Nguyen, D.D.; Lee, C.-J. Effect of Torrefaction on Steam Gasification of Biomass in Dual Fluidized Bed Reactor—A Process Simulation Study. *BioEnergy Res.* **2019**, *12*, 1042–1051. [CrossRef]
26. Treusch, K.; Mauerhofer, A.M.; Schwaiger, N.; Pucher, P.; Müller, S.; Painer, D.; Hofbauer, H.; Siebenhofer, M. Hydrocarbon production by continuous hydrodeoxygenation of liquid phase pyrolysis oil with biogenous hydrogen rich synthesis gas. *React. Chem. Eng.* **2019**, *4*, 1195–1207. [CrossRef]

27. Doelle, K.; Bajrami, B. Sodium Hydroxide and Calcium Hydroxide Hybrid Oxygen Bleaching with System. *IOP Conf. Series Mater. Sci. Eng.* **2018**, *301*, 012136. [CrossRef]
28. Ranzi, E.; Cuoci, A.; Faravelli, T.; Frassoldati, A.; Migliavacca, G.; Pierucci, S.; Sommariva, S. Chemical Kinetics of Biomass Pyrolysis. *Energy Fuels* **2008**, *22*, 4292–4300. [CrossRef]
29. Debiagi, P.; Gentile, G.; Cuoci, A.; Frassoldati, A.; Ranzi, E.; Faravelli, T. A predictive model of biochar formation and characterization. *J. Anal. Appl. Pyrolysis* **2018**, *134*, 326–335. [CrossRef]
30. Oyedun, A.; Patel, M.; Kumar, M.; Kumar, A. The Upgrading of Bio-Oil via Hydrodeoxygenation. In *Chemical Catalysts for Biomass Upgrading*; Wiley: New York, NY, USA, 2019.
31. Lazzari, E.; Schena, T.; Marcelo, M.C.A.; Primaz, C.T.; Silva, A.N.; Ferrão, M.F.; Bjerk, T.; Caramão, E.B. Classification of biomass through their pyrolytic bio-oil composition using FTIR and PCA analysis. *Ind. Crops Prod.* **2018**, *111*, 856–864. [CrossRef]
32. Elliott, D.C.; Meier, D.; Oasmaa, A.; van de Beld, B.; Bridgwater, A.V.; Marklund, M. Results of the International Energy Agency Round Robin on Fast Pyrolysis Bio-oil Production. *Energy Fuels* **2017**, *31*, 5111–5119. [CrossRef]
33. Zadeh, Z.E.; Abdulkhani, A.; Saha, B. Characterization of Fast Pyrolysis Bio-Oil from Hardwood and Softwood Lignin. *Energies* **2020**, *13*, 887. [CrossRef]
34. Liaw, S.-S.; Wang, Z.; Ndegwa, P.; Frear, C.; Ha, S.; Li, C.-Z.; Garcia-Perez, M. Effect of pyrolysis temperature on the yield and properties of bio-oils obtained from the auger pyrolysis of Douglas Fir wood. *J. Anal. Appl. Pyrolysis* **2012**, *93*, 52–62. [CrossRef]
35. Cao, X.; Pignatello, J.J.; Li, Y.; Lattao, C.; Chappell, M.A.; Chen, N.; Miller, L.F.; Mao, J. Characterization of Wood Chars Produced at Different Temperatures Using Advanced Solid-State ^{13}C NMR Spectroscopic Techniques. *Energy Fuels* **2012**, *26*, 5983–5991. [CrossRef]
36. Roger, R.P.M.A.T.; Rowell, M. *Handbook of Wood Chemistry and Wood Composites*; CRC Press: Boca Raton, FL, USA, 2012.
37. Barisano, D.; Canneto, G.; Nanna, F.; Villone, A.; Fanelli, E.; Freda, C.; Grieco, M.; Cornacchia, G.; Braccio, G.; Marcantonio, V.; et al. Investigation of an Intensified Thermo-Chemical Experimental Set-Up for Hydrogen Production from Biomass: Gasification Process Performance—Part I. *Processes* **2021**, *9*, 1104. [CrossRef]
38. Fermoso, J.; Rubiera, F.; Chen, D. Sorption enhanced catalytic steam gasification process: A direct route from lignocellulosic biomass to high purity hydrogen. *Energy Environ. Sci.* **2012**, *5*, 6358–6367. [CrossRef]
39. Zhai, M.; Guo, L.; Wang, Y.; Zhang, Y.; Dong, P.; Jin, H. Process simulation of staging pyrolysis and steam gasification for pine sawdust. *Int. J. Hydrogen Energy* **2016**, *41*, 21926–21935. [CrossRef]
40. Puig-Gamero, M.; Argudo-Santamaria, J.; Valverde, J.; Sánchez, P.; Sanchez-Silva, L. Three integrated process simulation using aspen plus®: Pine gasification, syngas cleaning and methanol synthesis. *Energy Convers. Manag.* **2018**, *177*, 416–427. [CrossRef]
41. Begum, S.; Rasul, M.G.; Akbar, D.; Ramzan, N. Performance Analysis of an Integrated Fixed Bed Gasifier Model for Different Biomass Feedstocks. *Energies* **2013**, *6*, 6508–6524. [CrossRef]
42. Marcantonio, V.; Bocci, E.; Monarca, D. Development of a Chemical Quasi-Equilibrium Model of Biomass Waste Gasification in a Fluidized-Bed Reactor by Using Aspen Plus. *Energies* **2019**, *13*, 53. [CrossRef]
43. Savuto, E.; Di Carlo, A.; Steele, A.; Heidenreich, S.; Gallucci, K.; Rapagnà, S. Syngas conditioning by ceramic filter candles filled with catalyst pellets and placed inside the freeboard of a fluidized bed steam gasifier. *Fuel Process. Technol.* **2019**, *191*, 44–53. [CrossRef]
44. Moradi, R.; Marcantonio, V.; Cioccolanti, L.; Bocci, E. Integrating biomass gasification with a steam-injected micro gas turbine and an Organic Rankine Cycle unit for combined heat and power production. *Energy Convers. Manag.* **2020**, *205*, 112464. [CrossRef]
45. Catalano, J.; Guazzone, F.; Mardilovich, I.P.; Kazantzis, N.K.; Ma, Y.H. Hydrogen Production in a Large Scale Water–Gas Shift Pd-Based Catalytic Membrane Reactor. *Ind. Eng. Chem. Res.* **2012**, *52*, 1042–1055. [CrossRef]
46. Peters, J.F. Pyrolysis for Biofuels or Biochar?—A Thermodynamic, Environmental and Economic Assessment. Ph.D. Thesis, Universidad Rey Juan Carlos, Móstoles, Spain, 2017. [CrossRef]
47. Patel, M.; Kumar, A. Production of renewable diesel through the hydroprocessing of lignocellulosic biomass-derived bio-oil: A review. *Renew. Sustain. Energy Rev.* **2016**, *58*, 1293–1307. [CrossRef]
48. He, Z.; Wang, X. Hydrodeoxygenation of model compounds and catalytic systems for pyrolysis bio-oils upgrading. *Catal. Sustain. Energy* **2012**, *1*, 28–52. [CrossRef]
49. Mani, S.; Tabil, L.G.; Sokhansanj, S. Grinding performance and physical properties of wheat and barley straws, corn stover and switchgrass. *Biomass-Bioenergy* **2004**, *27*, 339–352. [CrossRef]

Disclaimer/Publisher's Note: The statements, opinions and data contained in all publications are solely those of the individual author(s) and contributor(s) and not of MDPI and/or the editor(s). MDPI and/or the editor(s) disclaim responsibility for any injury to people or property resulting from any ideas, methods, instructions or products referred to in the content.